J Pharmacol Sci 97, 361 – 368 (2005)

Journal of Pharmacological Sciences

Full Paper

Simultaneous Real-Time Detection of Initiator- and Effector-Caspase Activation by Double Fluorescence Resonance Energy Transfer Analysis

Hiroshi Kawai[1], Takuo Suzuki[1], Tetsu Kobayashi[1], Haruna Sakurai[2], Hisayuki Ohata[2], Kazuo Honda[2], Kazutaka Momose[2], Iyuki Namekata[3], Hikaru Tanaka[3], Koki Shigenobu[3], Ryu Nakamura[4], Takao Hayakawa[1], and Toru Kawanishi[1,*]

[1]*Division of Biological Chemistry and Biologicals, National Institute of Health Sciences, Tokyo 158-8501, Japan*
[2]*Department of Pharmacology, School of Pharmaceutical Sciences, Showa University, Tokyo 142-8555, Japan*
[3]*Department of Pharmacology, Toho University School of Pharmaceutical Sciences, Chiba 274-8510, Japan*
[4]*Carl Zeiss Co., Ltd., Tokyo 160-0003, Japan*

Received August 31, 2004; Accepted January 8, 2005

Abstract. Fluorescence resonance energy transfer (FRET) with green fluorescent protein (GFP) variants has become widely used for biochemical research. In order to expand the choice of fluorescent range in FRET analysis, we designed various color versions of the FRET-based probes for caspase activity, in which the substrate sequence of the caspase was sandwiched by donor and acceptor fluorescent proteins, and studied the potential of these color versions as fluorescent indicators. Six color versions were constructed by a combination of cyan fluorescent protein (CFP), GFP, yellow fluorescent protein (YFP), and DsRed. Real-time monitoring in single cells revealed that all probes could detect caspase activation during tumor necrosis factor (TNF)-α-induced cell death as a fluorescent change. GFP-DsRed and YFP-DsRed were as sensitive as CFP-YFP, and CFP-DsRed also showed a large fluorescent change. By using two probes, CFP-DsRed and YFP-DsRed, we carried out simultaneous multi-FRET analysis and revealed that the initiator- and effector-caspases were activated almost simultaneously in TNF-α-induced cell death. These findings may give experimental bases for the development of novel techniques to analyze multi-events simultaneously in single cells by using FRET probes in combination.

Keywords: fluorescence resonance energy transfer, green fluorescent protein, tumor necrosis factor-α, cell death, caspase

Introduction

Many probes for various physiological reactions have been developed with green fluorescent protein (GFP) variants by using a similar strategy as that used with cameleon, the Ca^{2+}-sensing fusion protein developed by Miyawaki et al. (1 – 9). The cameleon consists of cyan fluorescent protein (CFP), calmodulin, M13 peptide, and yellow fluorescent protein (YFP). This fusion protein senses Ca^{2+} as the change of fluorescence resonance energy transfer (FRET) efficiency between CFP and YFP. Calmodulin binds M13 in the presence of Ca^{2+}, which causes conformational change in cameleon, resulting in a change in the distance between and relative orientation of CFP and YFP. This change alters the FRET efficiency from CFP to YFP; therefore, Ca^{2+} can be monitored as the fluorescent change (1).

CFP and YFP are the most frequently used pair for analysis by FRET. This pair is suitable for FRET analysis because the spectral overlap between the emission of the donor protein (CFP) and the excitation of the acceptor protein (YFP) is sufficient for energy transfer, and their ranges of fluorescence are far apart enough to be separated by measuring devices such as fluorescent microscopy (10). However, there are limitations for the CFP-YFP pair. It is impossible, for example, to use the CFP-YFP FRET probe for simultaneous measurement with other probes that are made of GFP variants or have

*Corresponding author. FAX: +81-3-3700-9064
E-mail: kawanish@nihs.go.jp.

fluorescein structure. If more choice of FRET probes is available from wider fluorescence ranges, it would allow us to analyze multi-events simultaneously occurring in living cells.

In this paper, we developed caspase-sensors of various colors by using cyan, green, yellow, and red fluorescent proteins and assessed their ability to detect the caspase activation in living single cells. Based on the findings obtained, we tried to perform multi-event FRET analysis and clarify the temporal relationships between biochemical reactions during cell death.

Materials and Methods

Plasmid construction

Plasmid encoding CY-sensor, YFP-peptide-CFP, was generated as previously reported (11). The sequence encoding 11 amino acids at the C-terminus of YFP was eliminated in this construct. The C-terminal truncated forms of the CFP (or GFP) gene were generated by PCR with primers containing the NheI site or BspEI site and pECFP-C1 (or pEGFP-C1; Clontech, Palo Alto, CA, USA) as a template, and the restricted fragment was inserted into the NheI/BspEI sites of the CY-sensor to generate a plasmid carrying truncated CFP (or GFP) at the N-terminus. DsRed was generated from pDsRed2-C1 (Clontech) by PCR, at the AgeI/NotI sites, and the restricted fragment was inserted into the AgeI/NotI sites of the CY-sensor to generate a plasmid carrying DsRed2 at the C-terminus. CG-, CR-, GR-, and YR-sensors were generated with a combination of these elements. The AgeI/BsrGI fragment from pEGFP-C1 was inserted into the AgeI/BsrGI sites of the CY-sensor to generate the GY-sensor. All cloned sequences were verified by sequencing.

Cell culture and transfection

HeLa cells were cultured in DMEM (Sigma-Aldrich, St. Louis, MO, USA) supplemented with 100 units/ml of penicillin G, 100 μg/ml of streptomycin, and 10% fetal calf serum (Invitrogen Corp., Carlsbad, CA, USA). Plasmid encoding the sensor protein was transfected into HeLa cells using Effectene Transfection Reagent (Qiagen, Hilden, Germany) according to the manufacturer's instructions. After 12 – 24 h incubation with the transfection reagent, the cells were washed with PBS and cultivated on dishes suitable for assay in medium containing 500 μg/ml of G418 for an additional 1 – 3 days until the assay was performed.

Western blotting

Cells cultured in a plastic dish were washed with PBS and lysed with 1 × SDS loading buffer. The samples dissolved in 1 × SDS loading buffer were incubated at 95°C for 2 min, and then they were loaded onto SDS-polyacrylamide gels (10%). Proteins were separated at 20 mA and then blotted to PVDF membranes in Tris-glycine transfer buffer at 100 V for 2 h. The membrane was incubated with block ace (Dainippon Pharmaceutical, Osaka) for 1 h, anti-GFP peptide antibody (Clontech, diluted with 0.1 × block ace to 1:1,000) for 2 h, and anti-rabbit IgG horseradish peroxidase-conjugated secondary antibody (Chemicon International Inc., Temecula, CA, USA; diluted with 0.1 × block ace to 1:10,000) for 1 h. The membrane was washed with TBS-T 3 times for 5 min after the incubation with the antibody. All of these incubations were performed at room temperature. The membrane was developed with the ECL chemiluminescence detection reagent (Amersham Biosciences, Piscataway, NJ, USA).

Measurement of fluorescent spectra of the sensors in HeLa cells

Spectral imaging was performed with LSM510META (Carl Zeiss, Jena, Germany) (12). Cells expressing one of the sensors were observed by excitation light at 458 nm (Ar laser), emitted fluorescence was separated by a grating, and the separated fluorescence were detected by 24 photomultiplier tubes (PMT) that were set to detect fluorescence at 468 – 714 nm. Each PMT detected fluorescence in the 10.7-nm wavelength range. So, the fluorescent spectrum at 468 – 714 nm was obtained with 10.7-nm resolution. Cell death was induced by incubation with tumor necrosis factor (TNF)-α (100 ng/ml) and cycloheximide (CHX, 10 μg/ml) for 6 h. Fluorescent spectra of living and dead cells were obtained from the whole cell region of normal-shaped and spherical cells, respectively.

Real-time imaging with FRET sensors

Transfected cells were cultured on a cover glass (25-mm diameter, 0.15 – 0.18-mm thickness) for 1 – 3 days. Cells were treated with TNF-α/CHX and then incubated under the usual culture condition for 1 – 2 h before analysis. Analyses were carried out by confocal laser-scanning fluorescent microscopy using a Carl Zeiss LSM510 system. During the observation, the media were buffered with 10 mM hepes buffer (pH 7.4), and the cells were maintained at 35 – 37°C. DIC images and grayscale images for fluorescence channels were obtained every 2 min unless otherwise described. Excitation lights for the FRET probe (458 nm for the CG-, CY-, GY-, and CR-sensors; 488 nm for the GR- and YR-sensors) were provided by an Ar laser with a 458 or 488 dichroic mirror. Images of the FRET probe were obtained separately for both donor and acceptor

Table 1. Measurement conditions for real-time analysis by LSM510

Sensor	Fusion protein[a]	Excitation (nm)[b]	Emission (nm)[c]		
			beam splitter	emission filter	
				donor	acceptor
CG	GFP-peptide-CFP	458	515	467.5 – 497.5	515 – 545
CY	YFP-peptide-CFP	458	515	467.5 – 497.5	515 – 545
GY	YFP-peptide-GFP	458	515	475 – 525	515 – 545
CR	CFP-peptide-DsRed	458	515	467.5 – 497.5	560 – 615
GR	GFP-peptide-DsRed	488	545	505 – 530	560 – 615
YR	YFP-peptide-DsRed	488	545	505 – 530	560 – 615

[a]N-terminal CFP, GFP, and YFP were in a truncated form in which 11 amino acids at the C-terminus were eliminated, and His_{10} was present at the C-terminus of CG, CY, and GY. [b]Excitation light was obtained by Ar laser and a 458 or 488 dichroic mirror. [c]Emitted fluorescence was separated by a 515 or 545 dichroic mirror, and the fluorescence of the donor and that of the acceptor were obtained through band pass emission filters.

fluorescence using a dichroic mirror and band-pass emission filters as shown in Table 1. Images were processed and quantified using MetaFluor software as follows: The average pixel intensity of the fluorescence of the whole cell region was determined for each channel. The ratio value was calculated as the average pixel value of the fluorescent ratio, (fluorescent intensity for the acceptor channel) / (fluorescent intensity for the donor channel), in the whole cell region. As cells changed their morphology during the observation, the whole cell region was determined separately in each image.

Results

Construction and characterization of FRET probes

We developed plasmids expressing caspase sensors as shown in Fig. 1a. A 12-amino-acid peptide derived from poly(ADP-ribose)polymerase (PARP) that is a well-known substrate of effector caspases was sandwiched by two different fluorescent proteins (an example of CFP-YFP is shown in Fig. 1a). The peptide sequence contains a caspase recognition site in the middle, and this fusion protein was cleaved mainly by caspase-3 (11). CFP-GFP, CFP-YFP, GFP-YFP, CFP-DsRed, GFP-DsRed, and YFP-DsRed were used as the donor-acceptor pairs. We named these fusion proteins CG-, CY-, GY-, CR-, GR-, and YR-sensor, respectively (Table 1). These fusion proteins show FRET in their intact form, whereas in the presence of active caspase, the peptide sequence is cleaved, CFP and YFP are far apart, and the fusion proteins do not show FRET any longer. The fluorescent ratio of acceptor/donor reflects the amount of FRET, so we used the reduction of this value as an index of caspase activation.

HeLa cells expressing one of these fusion proteins

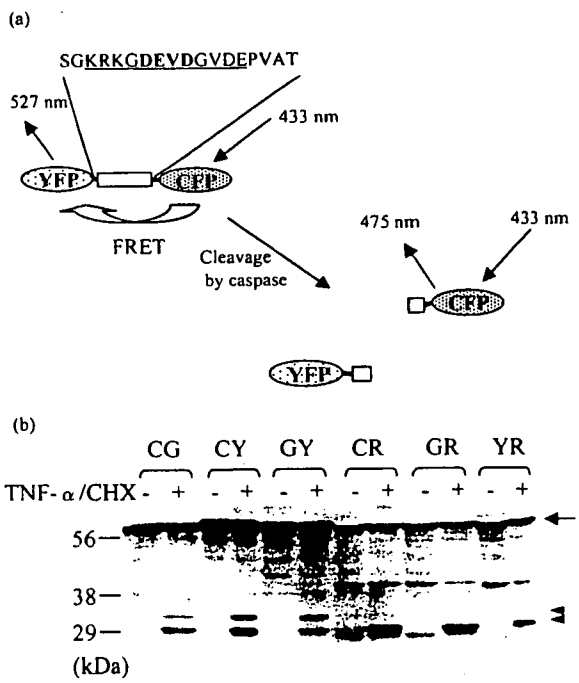

Fig. 1. Small peptide sandwiched by two different fluorescent proteins can be a caspase-sensor. a: Fusion protein that consists of a PARP-derived 12-amino-acid peptide sandwiched by CFP and YFP exhibits FRET in its intact form. In the presence of active caspases, the peptide is cleaved, and the fusion protein does not exhibit FRET. Caspase activation can be detected by measuring the fluorescence of CFP and YFP. b: Six caspase-sensors expressed in HeLa cells were cleaved by cell death stimuli. HeLa cells expressing one of the sensors were incubated in the presence or absence of TNF-α/CHX for 6 h. The arrow and arrowhead indicate the full length and cleaved fragments of the sensors.

were treated with TNF-α/CHX. After 6-h exposure, the sensor proteins in cells were extracted and analyzed by western blotting. All 6 fusion proteins were detected in their intact forms in non-treated HeLa cells (arrow in Fig. 1b), and small fragments were detected in cells treated with TNF-α/CHX (arrowhead in Fig. 1b), indicating that the fusion proteins were cleaved by cell death stimuli, as expected. The antibody used in this analysis reacts with CFP, GFP, and YFP, but not with DsRed. Therefore, CG-, CY-, and GY-sensor showed two cleaved fragments corresponding to the N- and C-terminal C/G/YFP, whereas CR-, GR-, and YR-sensor showed only one cleaved fragment corresponding to the N-terminal C/G/YFP.

Figure 2 shows the fluorescent spectra of the probes in living or dead cells. Comparing the fluorescence of living and dead cells, all sensors showed an increase of donor fluorescence and/or a reduction of acceptor fluorescence in response to cell death stimuli. This change results in a reduction of fluorescent ratio of acceptor/donor that is an index of FRET. These sensors were designed to show a reduction of FRET with caspase activation, so these results suggest that all 6 fusion proteins work as expected and can detect caspase activation as fluorescent change in living cells.

For simultaneous application of two or more fluorescent probes, minimum spectral overlap between probes is one of the important conditions. The spectra in Fig. 2 give us a clue to determine a suitable combination of probes for multi-probe analysis. CG-, CY-, or GY-sensor has the least fluorescence in the red-fluorescence region (>600 nm), so it is possible to use this fluorescent region for another dye. We can use a red-fluorescent dye that has fluorescence in this region together with CG-, CY-, or GY-sensor simultaneously. On the other hand, YR-sensor has the least fluorescence in the blue-cyan region (<500 nm), so blue-cyan-fluorescent dye is applicable with this probe for the purpose of simultaneous fluorescence imaging. The color variations of FRET probe may be useful for multi-probe analysis.

Real-time detection of caspase activation in living cells

Next, we applied the sensor proteins to real-time measurement. HeLa cells expressing one of the sensor proteins were analyzed with a time resolution of 2 min by laser-scanning confocal fluorescent microscopy. Figure 3 shows typical images (a) and fluorescent changes (b) during cell death. HeLa cells expressing GR-sensor were treated with TNF-α/CHX. An increase of donor protein fluorescence (GFP), a reduction of acceptor protein fluorescence (DsRed), and a reduction of the fluorescent ratio of acceptor/donor (DsRed/GFP) were observed in each cell at a different time. Caspases began to work at the point when the fluorescent ratio began to decrease.

All sensors showed similar changes, meaning that all sensors were useful for real-time detection of the caspase activation in a living cell, although the apparent sensitivity was different between sensors. In order to compare the sensitivity of these sensors to detect the caspase activation, the amount of the fluorescent change was calculated. We defined the start point and the end

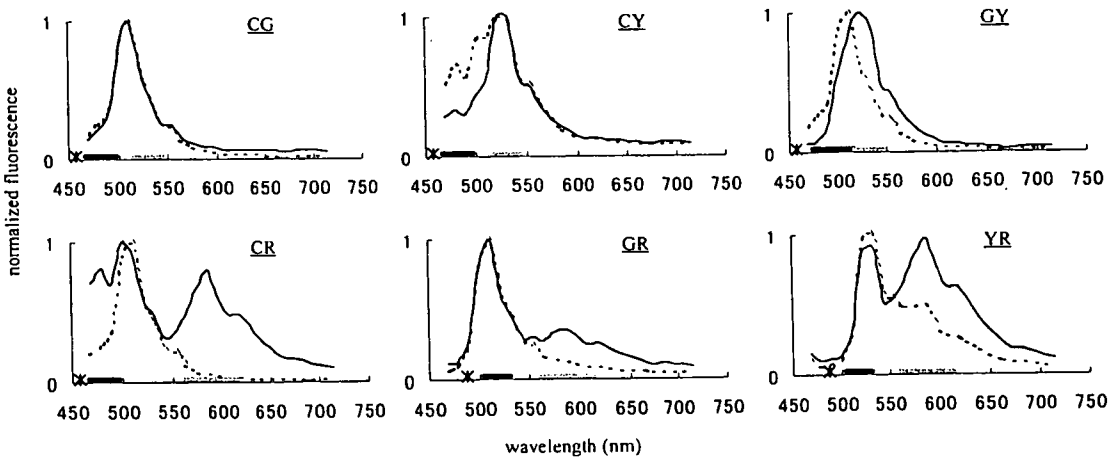

Fig. 2. Fluorescent spectra of the caspase-sensors in HeLa cells. HeLa cells expressing each sensor were treated with TNF-α/CHX for 6 h. The spectra of living cells (solid line) and dead cells (dotted line) were obtained from normal-shaped and spherical cells, respectively. Each spectrum was normalized to the peak that showed maximal intensity. The asterisks and bars on horizontal axes represent the excitation wavelength and detection range for the emitted fluorescence, respectively, used in real-time imaging analysis. Each spectrum is the average of data from 13 - 26 cells.

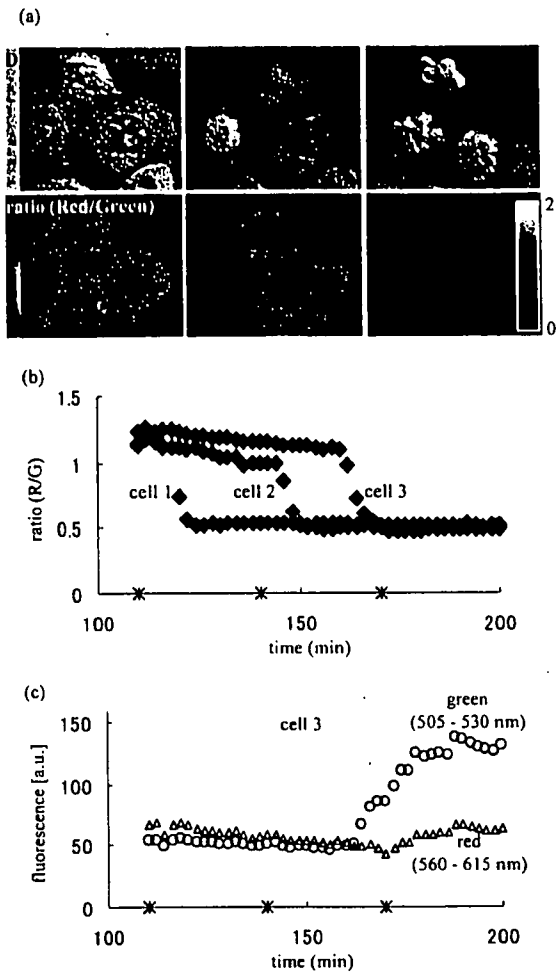

Fig. 3. Real-time imaging of caspase activation in living HeLa cells during cell death. HeLa cells expressing GR-sensor were treated with TNF-α/CHX, and fluorescent images were obtained every 2 min. a: DIC images (upper panels) and fluorescent ratios (Red/Green, lower panels) are shown in grayscale. The indicated time represents the time after the addition of TNF-α/CHX. Scale bar, 10 μm. b: The fluorescent ratio of cells were plotted. Cell 1, 2, or 3 corresponds to the cells shown in panel a. c: The mean pixel intensity in arbitrary fluorescent units (a.u.) for each channel was plotted. The fluorescence of cell No. 3 from panel a is shown. Open circle, GFP; open triangle, DsRed; closed diamond, ratio of Red/Green. Asterisks on the x-axis indicate the time points of the images in panel a.

point of the reduction of the fluorescent ratio as follows: the start point was the point after which the value decreased over four continuous points or more, the value decreased more than 10% in total, and the reduction of the value was not because of artificial noise such as focus shift; the end point followed the start point and was the point at which the value stopped decreasing. The sensitivity of the probe was calculated as $\Delta R = |(R_{end} - R_{start}) / R_{start}|$, where R_{start} and R_{end} were the fluorescent ratio at the start point and the end point, respectively. Figure 4 shows ΔR for each probe. GR and YR, as well as CY, showed the highest ΔR. They each showed a more than 50% change during cell death. CR showed a slightly lower ΔR, but its change was still 44% on average. CG and GY were less sensitive, probably because the fluorescent spectra of the donor and the acceptor were so similar that our system could not effectively measure FRET between them. CY *vs* GR, CY *vs* YR, or GR *vs* YR were not significantly different, and any other comparisons were significantly different by the Games-Howell test ($P<0.05$).

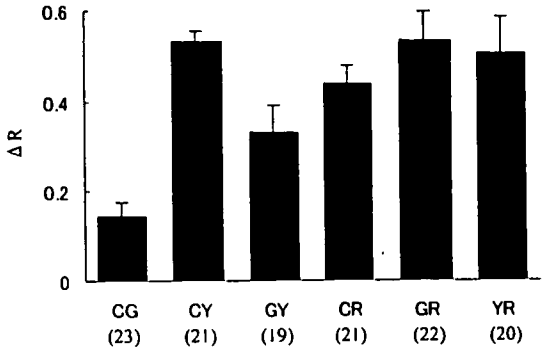

Fig. 4. Comparison of the sensitivity of various caspase-sensors. The amount of change of the fluorescent ratio during cell death (ΔR) was determined in each cell as described in the text. Bars represent means ± S.D. The number of cells used in each analysis is shown in parentheses.

Simultaneous multi-event analysis using two FRET probes

Finally, we tried to perform multi-FRET measurement. We constructed a YR-initiator caspase sensor and a CR-effector caspase sensor by changing the caspase substrate sequence in the sensor and applied them to real-time imaging analysis simultaneously in order to reveal the temporal relationships between the initiator caspase activation and the effector caspase activation in the same cell. The caspase substrate sequences were derived from procaspase-3 and PARP, respectively, and their sequences are shown in Fig. 5a. These sensors were cleaved mainly by caspase-8/9 and caspase-3, respectively (11).

Simultaneous measurement of these sensors was performed under the multi-track scanning mode, in which two sets of excitation-detection conditions were used alternatively. CFP fluorescence by excitation at 458 nm was measured in the first track, and YFP and DsRed fluorescence by excitation at 488 nm was mea-

(a) YFP-SGLDCGIETDSGVDEPVAT-DsRed : YR-(IC)sensor
CFP-SGKRKGDEVDGVDEPVAT-DsRed : CR-(EC)sensor

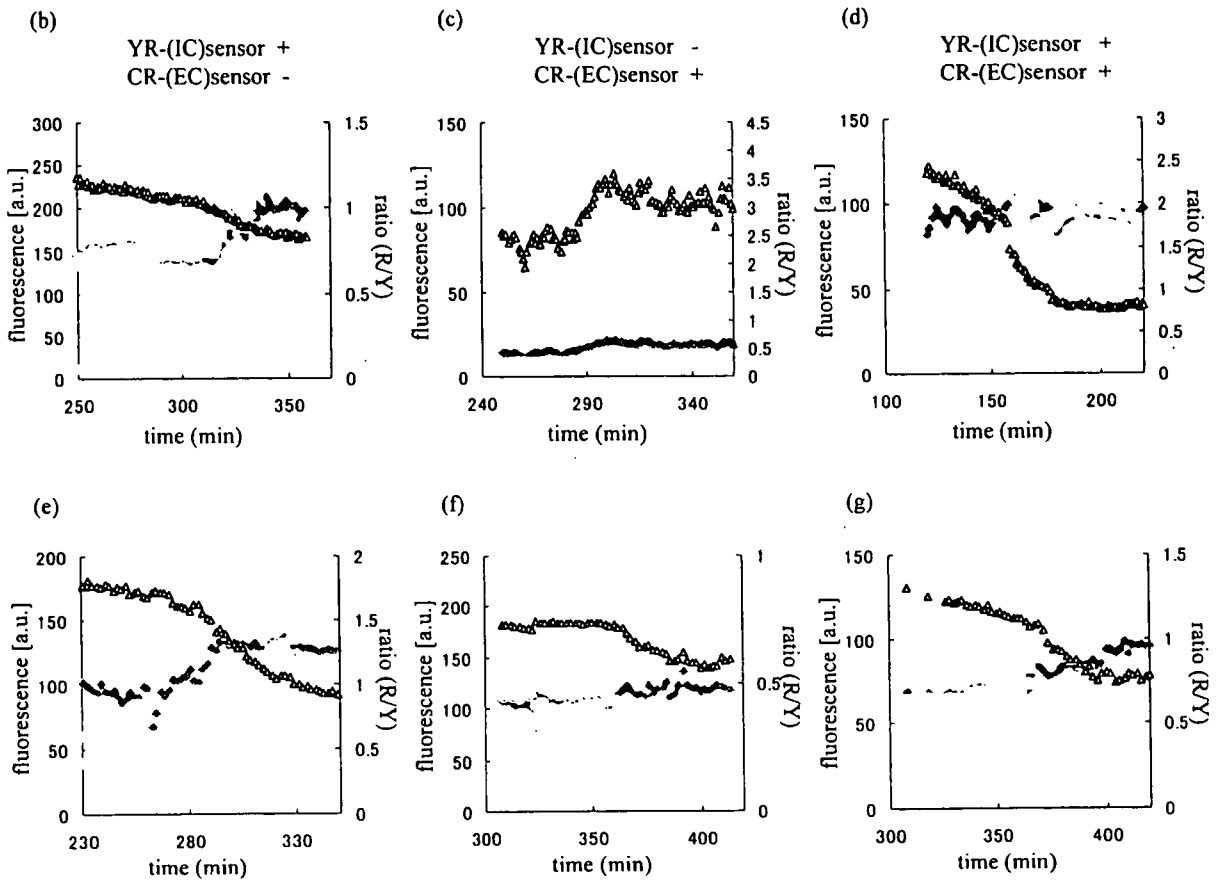

Fig. 5. Simultaneous measurement of initiator- and effector-caspase activation with YR-sensor and CR-sensor. HeLa cells expressing YR-initiator caspase sensor and/or CR-effector caspase sensor were treated with TNF-α/CHX and observed as described in the text. a: Probes used in this study. Underline indicates peptide derived from procaspase-3 and PARP, and bold indicates the consensus 4 amino acid sequence for caspase recognition. b – g: Cells expressing YR-initiator caspase sensor (b), CR-effector caspase sensor (c), or both of them (d – g) were treated with TNF-α/CHX. The fluorescence of CFP, YFP, and DsRed (colored plots) and the fluorescent ratio of DsRed/YFP (open triangles) were plotted against time after TNF-α/CHX treatment.

sured in the second track. The time difference of scanning between tracks is about 3 – 8 s. Figures 5b and 5c show control studies with cells expressing only one of the probes. These control studies were conducted in the same conditions as Fig. 5d. Figures 5b and 5c indicate that the YR- and CR-sensor could detect initiator- and effector-caspase activation as an increase of YFP and CFP signal, respectively, and the contamination of the signal between the YFP and CFP channels was negligible. So, we used an increase of the YFP and CFP signal as index of the initiator- and the effector-caspase activation, respectively. The DsRed signal in Fig. 5c was derived from direct excitation of DsRed in the CR-sensor by the excitation light at 488 nm and was increased when the cell shrank because fluorescent proteins were concentrated in the cell.

Figure 5d shows typical data of multi-probe analysis with the YR-initiator caspase sensor and CR-effector caspase sensor. In this cell, the fluorescence was dramatically changed at 150 – 160 min after TNF-α /CHX treatment. The YFP and CFP signal began to increase almost simultaneously, suggesting that initiator caspase and effector caspase were initially activated within a short time period. Figures 5e – 5g show three

other examples. We observed more than 30 cells in at least 3 independent experiments and found that all dying cells showed similar results.

Discussion

In this study, we developed various color versions of caspase-sensors with CFP, GFP, YFP, and DsRed and revealed that various combinations are applicable in FRET analysis. CY, CR, GR, and YR pairs are preferable FRET pairs that possess a high ability to detect the caspase activation.

The sensitivity shown in Fig. 4 represents the apparent FRET change that depends on the measuring system and was determined by three factors. 1) Intrinsic FRET efficiency: All 4 fluorescent proteins had different fluorescent characteristics; therefore, the levels of FRET efficiency in 6 probes differed from each other. 2) Excitation crosstalk: The acceptors were excited directly by the excitation light. 3) Emission crosstalk: The acceptor channel was contaminated with the donor signal, and vice versa, because the setting shown in Table 1 could not perfectly separate the signals from the donor and the acceptor. The differences in these factors cause the difference of sensitivity among the sensors. Factors 2) and 3) reduce the apparent FRET change in the measurement. In the case of the CG-sensor, for example, fluorescent spectrum of donor and acceptor are so similar that the intrinsic FRET efficiency may be high, but excitation and emission crosstalk may also be high, much higher than in other sensors (e.g., CY-sensor), resulting in the relatively low sensitivity of this probe in our measurement system. Crosstalk effects are undesirable for detection, but it is impossible to completely eliminate these effects in the current measurement system. Maybe we could obtain different results by using spectral imaging in which emission crosstalk is eliminated (12).

According to the characteristics of the fluorescence spectrum, the CY probe seems to be one of the best for FRET-detection. However, the probe is not suitable for imaging with confocal laser microscopy, because the normal argon ion laser, the most common one in confocal microscopes, is not suitable for the excitation of CFP. The blue laser is the most suitable for the excitation, but it is not common in confocal laser microscopes. In this paper, we had to use the argon ion laser emitting 458 nm and the special emission filters optimized for the confocal ratio-imagings of caspase activation using the CY probe (11). On the contrary, the GR probe and the YR probe can be efficiently excited at 488 nm emitted by the normal argon ion laser and imaged with a set of emission filters for fluorescein and a set for rhodamine, with which almost all of the confocal microscopes are equipped. In addition, the GR probe is useful for the detection of caspase activation in flow cytometry, because almost all of the normal flow cytometers are also usually equipped with the laser and the emission filters.

DsRed-containing "red"-sensors have several characteristics that are different from other "non red"-sensors. As previously reported (13), it takes longer for DsRed to mature and emit red fluorescence than it takes for GFPs, and DsRed fluorescence tends to decrease during real-time observation, which may cause a reduction of the apparent sensitivity. These characteristics must be considered when any analysis is performed with these sensors, but as shown in Figs. 4 and 5, red-sensors have a potential similar to that of the CY-sensor and are very useful for multi-color imaging.

It has been reported that DsRed is useful as a fusion tag and a partner for FRET (13, 14). Erickson et al. analyzed the potential of DsRed as a FRET partner with CFP and GFP (14). Mizuno et al. developed a Ca^{2+} sensing fusion protein using Sapphire and DsRed (13). And recently, Karasawa et al. used two novel fluorescent proteins, namely the cyan-emitted and orange-emitted fluorescent proteins from *Acropara* sp. and *Fungia concinna*, respectively, as a FRET pair, and measured caspase-3 activity in cells (15). These results combined with our results indicate that various fluorescent proteins including GFP derivatives, DsRed, and others are useful for FRET analysis. By choosing the appropriate two fluorescent proteins as the FRET pair, we can customize the fluorescent range of FRET-based imaging probes to fit the analysis, which would expand the flexibility of simultaneous multi-event analysis.

By using the CR and YR developed in this study, we were able to analyze two FRET probes simultaneously in the same cells. In several reports, the initiator caspase activity and the effector caspase activity were measured in living cells (8, 9, 11). In these reports, however, each activity was measured independently in different cells. To our knowledge, the present study is the first report that analyzes these activities in the same cell. The results directly reveal the temporal relationships between these caspase activities. It takes a long time for cells to start the initiator caspase activation after drug treatment, but it takes a relatively short time for cells to start the effector caspase activation after the initiator caspase activation. The caspase cascade is initiated at the last stage of cell death signaling, and it proceeds within a short time period.

Acknowledgments

This study was supported in part by a Grant-in-Aid for

Research on Health Sciences Focusing on Drug Innovation from the Japan Health Science Foundation; a Grant-in-Aid for Research on Advanced Medical Technology from the Ministry of Health, Labour, and Welfare; and a grant (MF-16) from the Organization for Pharmaceutical Safety and Research.

References

1 Miyawaki A, Llopis J, Heim R, Mccaffery JM, Adams JA, Ikura M, et al. Fluorescent indicators for Ca^{2+} based on green fluorescent proteins and calmodulin. Nature. 1997;388:882–887.
2 Zaccolo M, Giorgi FD, Cho CY, Feng L, Knapp T, Negulescu PA, et al. A genetically encoded, fluorescent indicator for cyclic AMP in living cells. Nat Cell Biol. 2000;2:25–29.
3 Nagai Y, Miyazaki M, Aoki R, Zama T, Inouye S, Hirose K, et al. A fluorescent indicator for visualizing cAMP-induced phosphorylation in vivo. Nat Biotechnol. 2000;18:313–316.
4 Kurokawa K, Mochizuki N, Ohba Y, Mizuno H, Miyawaki A, Matsuda M. A pair of fluorescent resonance energy transfer-based probes for tyrosine phosphorylation of the CrkII adaptor protein in vivo. J Biol Chem. 2001;276:31305–31310.
5 Sato M, Ozawa T, Inukai K, Asano T, Umezawa Y. Fluorescent indicators for imaging protein phosphorylation in single living cells. Nat Biotechnol. 2002;20:287–294.
6 Tyas L, Brophy VA, Pope A, Rivett AJ, Tavare JM. Rapid caspase-3 activation during apoptosis revealed using fluorescence-resonance energy transfer. EMBO Rep. 2000;1:266–270.
7 Rehm M, Dussmann H, Janicke RU, Tavare JM, Kogel D, Prehn JHM. Single-cell fluorescence resonance energy transfer analysis demonstrates that caspase activation during apoptosis is a rapid process: role of caspase-3. J Biol Chem. 2002;277:24506–24514.
8 Luo KQ, Yu VC, Pu Y, Chang DC. Measuring dynamics of caspase-8 activation in a single living HeLa cell during TNFα-induced apoptosis. Biochem Biophys Res Commun. 2003;304:217–222.
9 Takemoto K, Nagai T, Miyawaki A, Miura M. Spatio-temporal activation of caspase revealed by indicator that is insensitive to environmental effects. J Cell Biol. 2003;160:235–243.
10 Tsien RY. The green fluorescent protein. Annu Rev Biochem. 1998;67:509–544.
11 Kawai H, Suzuki T, Kobayashi T, Mizuguchi H, Hayakawa T, Kawanishi T. Simultaneous imaging of initiator/effector caspase activity and mitochondrial membrane potential during cell death in living HeLa cells. Biochim Biophys Acta. 2004;1693:101–110.
12 Zimmermann T, Rietdorf J, Pepperkok R. Spectral imaging and its applications in live cell microscopy. FEBS Lett. 2003;546:87–92.
13 Mizuno H, Sawano A, Eli P, Hama H, Miyawaki A. Red fluorescent protein from Discosoma as a fusion tag and a partner for fluorescence resonance energy transfer. Biochemistry. 2001;40:2502–2510.
14 Erickson MG, Moon DL, Yue DT. DsRed as a potential FRET partner with CFP and GFP. Biophys J. 2003;85:599–611.
15 Karasawa S, Araki T, Nagai T, Mizuno H, Miyawaki A. Cyan-emitting and orange-emitting fluorescent proteins as a donor/acceptor pair for fluorescence resonance energy transfer. Biochem J. 2004;381:307–312.

J. Biochem. 137, 579–586 (2005)
DOI: 10.1093/jb/mvi070

Thrombomodulin Enhances the Invasive Activity of Mouse Mammary Tumor Cells

Shingo Niimi[1,*], Mizuho Harashima[2], Kazuko Takayama[2], Mayumi Hara[2], Masashi Hyuga[1], Taiichiro Seki[2], Toyohiko Ariga[2], Toru Kawanishi[1] and Takao Hayakawa[3]

[1]Division of Biological Chemistry and Biologicals, National Institute of Health Sciences, Kamiyoga 1-18-1, Setagaya-ku, Tokyo 158-8501; [2]Department of Nutrition and Physiology, Nihon University College of Bioresource Sciences, Kameino, Fujisawa 252-8510; and [3]Deputy Director General, National Institute of Health Sciences, Kamiyoga 1-18-1, Setagaya-ku, Tokyo 158-8501

Received January 31, 2005; accepted February 18, 2005

Thrombomodulin (TM) is a thrombin receptor on the surface of endothelial cells that converts thrombin from a procoagulant to an anticoagulant. Thrombin promotes invasion by various tumor cells, and positive or negative correlations are found between the expression of TM and tumorigenesis in some patients. In this study, we used an invasion assay to investigate the effect of TM on the invasive activity of a mouse mammary tumor cell line, MMT cells, and the effects of TM were compared with those of thrombin as a positive control. In the presence of 1% fetal calf serum (FCS), TM significantly stimulated MMT cell invasion in a dose-dependent manner, resulting in an approximately 3-fold increase at 1–10 pg/ml over the untreated control. Thrombin also caused a similar degree of stimulation at 50 ng/ml. Since thrombin activity was detected in the components of the assay system, an invasion assay was also performed in a thrombin-activity-depleted assay system constructed to eliminate the effect of thrombin activity; TM (10 pg/ml) plus thrombin (1 pg/ml) stimulated invasion by approximately 3.5-fold in this assay system. Hirudin, a specific thrombin inhibitor, inhibited stimulation by TM as well as by thrombin in both the presence and absence of 1% FCS. Investigations of the effects of TM on proliferation, adhesion and chemotaxis to clarify the mechanism of stimulation by TM revealed that TM does not affect proliferation or adhesion in the presence of 1% FCS, but stimulates chemotaxis by approximately 2.3-fold. Similar results were obtained in experiments using thrombin. TM (10 pg/ml) plus thrombin (1 pg/ml), on the other hand, stimulated chemotaxis by approximately 2.3-fold in the thrombin-activity-depleted assay system. Binding studies using [^{125}I]-thrombin revealed that the cells have specific saturable binding sites for thrombin. These results show that TM stimulates the invasive activity of MMT cells, probably by acting as a cofactor for the thrombin-stimulated invasion of the cells *via* its receptor and lowering the effective concentration of thrombin. The findings also indicate that the stimulation of invasive activity in the presence of 1% FCS and in the thrombin-activity-depleted assay system may mainly be mediated by the stimulation of chemotaxis.

Key words: invasion, thrombin, thrombomodulin.

Abbreviations: TM, thrombomodulin; MEM, modified Eagle's medium; CS, calf serum; FCS, fetal calf serum; MMP, matrix metalloprotease; ECM, extracellular matrix; Boc-Asp(Obzl)-pro-Arg-MCA, Boc-β-benzyl-Asp-Pro-Arg-4-methyl-coumaryl-7-amide; PBS, phosphate-buffered saline.

Thrombomodulin (TM) is a thrombin receptor on the surface of endothelial cells (*1*) that was first discovered as a cofactor for the thrombin-catalyzed activation of the anticoagulant protein C (*2*). Biologically active soluble forms of TM, which probably represent the products of limited proteolytic cleavage of cell-surface TM, were later detected in human plasma (*3*), suggesting a possible role of the soluble forms *in vivo*. TM also positively or negatively regulates various functions of thrombin as described below. TM stimulates the inactivation of pro-urokinase-type plasminogen activator (*4*), the activation of TAF I (*5*), and the activation of progelatinase A (*6*). TM inhibits the activation of platelets (*7*), the activation of factor X (*8*) and human endothelial cells (*9*), the stimulation of fibrin formation (*8*), and the proliferation of arterial smooth muscle cells (*10*) and human umbilical vein endothelial cells (*11*).

On the other hand, there are several direct and indirect lines of evidence indicating that thrombin stimulates invasion and/or metastasis by tumor cells (*12–18*), and it has recently been reported that the expression of TM is increased or decreased in some carcinomas. The expression of TM increases in squamous carcinomas of the lung (*19*), colorectal carcinomas (*20*), and some transitional

*To whom correspondence should be addressed. Tel: +81-3-3700-9347, Fax: +81-3-3700-9084, E-mail: niimi@nihs.go.jp

carcinomas (*21–22*), and its expression level is negatively correlated with the malignancy of carcinoma of the esophagus (*23*), hepatocellular carcinoma (*24*), and ovarian tumors (*25*). There is also evidence of increased serum levels of TM in some tumors, including pancreatic cancer (*26*), digestive tract carcinoma (*27*), and glioblastoma (*28*). Based on this evidence, it is likely that TM plays some role in the regulation of tumor metastasis.

In this study, we investigated the effects of TM on the invasive activity of a mouse mammary tumor cell line, MMT, by an *in vitro* invasion assay, because tumor cell invasion through the basement membrane is a critical step in the process of metastasis (*29–30*). We also compared the effects of TM with those of thrombin as a positive control.

MATERIALS AND METHODS

Materials—TM was a kind gift of Asahi Kasei Pharma, Japan. The TM was prepared as described by Gomi *et al.* (*31*). Plasmids containing the cDNA encoding TM (residues 1–498) were transfected into COS-1 cells, and the recombinant TM was purified from serum-free COS-1-cell-conditioned medium. The purified TM yielded a single band at 90 kDa in SDS-PAGE under reducing conditions. The recombinant TM was confirmed to be thrombin-free by a protein C activating assay developed in our laboratory (*32*). Thrombin (1,140 units/mg protein) was a kind gift of Mochida Pharmaceutical Co., Ltd., Japan. Hirudin was purchased from Wako (Osaka, Japan). A fluorogenic substrate, Boc-β-benzyl-Asp-Pro-Arg-4-methyl-coumaryl-7-amide (Boc-Asp(Obzl)-pro-Arg-MCA), was purchased from Peptide Institute, Inc. (Osaka, Japan).

Cell Culture—MMT mouse mammary tumor cells were obtained from the Japanese Health Science Research Resource Bank and cultured in modified Eagle's medium (MEM) supplemented with 10% calf serum (CS) on 60-mm diameter culture dishes, 4×10^5 cells per dish. After 7 d, the subconfluent MMT cells were detached from the culture dishes with 0.25% trypsin/EDTA, treated with MEM containing 10% CS, and collected by centrifugation. The cells were then washed with MEM and used in experiments. In some experiments, the thrombin activity associated with cells was depleted as described below, and the resultant cells were used for various experiments in which MEM containing 0.1% BSA was used as the basal medium. We refer to this assay system as the thrombin-activity-depleted assay system below. To deplete thrombin activity, the cell suspension (1.5×10^5 cells in 10 ml of MEM) was incubated in a non-adherent form on 100-mm diameter non-treated culture dishes pre-coated with BSA (10 mg/ml) for 2 h in a humidified chamber at 37°C under 5% CO_2, and then washed with MEM.

In Vitro Invasion Assay—In vitro invasion by MMT cells was measured in a Matrigel invasion chamber (Collaborative Biomedical Products, Bedford, MA, USA). The chamber (upper compartment) was placed in a 24-well culture plate (lower compartment), and the cell suspension (1.6×10^5 cells in 500 μl) and the basal medium (750 μl) containing various factors were added to the upper and lower compartments, respectively. MEM containing 1% fetal calf serum (FCS) or 0.1% BSA was used as the basal medium. Matrigel invasion chambers were pre-coated with fibronectin as described below before use in the thrombin-activity-depleted assay system. Human plasma fibronectin solution (IWAKI, Japan) was diluted to a final concentration of 5 μg/ml with phosphate-buffered saline (PBS), and a 300 μl aliquot was added to the chamber and a 750 μl aliquot to the 24-well culture plate. The chamber and 24-well plate were allowed to stand at 37°C for 2 h and were then washed with PBS. After incubating the cells for 18 h, the filters were fixed with methanol and stained with hematoxylin and eosin. The cells on the upper surface of the filters were removed by wiping with cotton swabs, and the number of cells that had migrated to the lower surface of the filters was counted under a microscope.

Measurement of Thrombin Activity—Thrombin activity in FCS, CS, and on cells was measured by the method of Kawabata *et al.* (*33*). A 10 μl volume of 10% FCS or CS was mixed with 90 μl of reaction buffer containing 50 mM Tris-HCl, pH 8.0, 100 mM NaCl, and 10 mM $CaCl_2$, with or without hirudin (0.5 unit/ml). Packed cells (1×10^6 cells) were suspended in 100 μl of reaction buffer with or without hirudin (0.5 unit/ml). After adding 1 μl of 10 mM substrate, Boc-Asp(Obzl)-pro-Arg-MCA solution to the cell suspension, the mixture was incubated for 20 min at 37°C, and the reaction was stopped by adding 600 μl of 0.6 M acetic acid. The fluorescence of the aminomethyl-coumarine released was measured with a fluorospectrophotometer at an excitation wavelength of 380 nm and an emission of 460 nm. A blank solution was prepared by adding 1 μl of substrate solution to the reaction buffer mixed with 600 μl of 0.6 M acetic acid. Thrombin activity was calculated using 1, 2.5, 5 and 10 ng/ml thrombin solutions as standards and subtracting the fluorescence obtained in the presence of hirudin from that in the absence of hirudin. A linear dose-response curve was obtained between 0.5–5 ng/ml of thrombin, and its activity was inhibited by more than 98% by hirudin (0.5 unit/ml). The fluorescence of each sample was within the linear range.

Proliferation Assay—The cell suspension (1×10^5 cells in 4 ml) was seeded on 60-mm diameter culture dishes and incubated with each factor for 18 h. MEM containing 1% FCS was used as the basal medium. The cells were then detached from the culture dishes with 0.25% trypsin/EDTA, treated with MEM containing 10% CS, collected by centrifugation, and counted with a hemocytometer.

Adhesion Assay—Adhesion assays were performed by a modification of the method of Deryugina *et al.* (*34*). A 300 μl aliquot of fibronectin (5 μg/ml), prepared as described above, was added to each well of 24-well plates (IWAKI, Japan). The plates were allowed to stand overnight at 4°C, washed with PBS, blocked with 1% BSA in PBS for 1 h at 37°C, and finally washed in PBS. MMT cells (55×10^4 cells) were exposed to each factor in 2 ml of MEM containing 1% FCS for 30 min at 37°C. After washing with 2 ml of MEM, the cell suspensions (1×10^5 cells in 0.38 ml of MEM) were seeded on each well. After incubation for 30 min at 37°C, non-adherent cells were removed by washing with PBS, and the adherent cells were fixed and stained with 0.2% crystal violet in 10% ethanol for 10 min. After three washes with 2 ml of PBS,

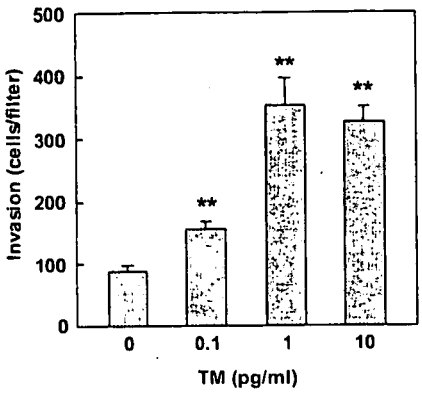

Fig. 1. **Dose dependency of the effect of TM on invasiveness.** MEM containing 1% FCS was used as the basal medium. The concentrations of TM indicated are the concentrations in the lower compartment. The data shown are means ± SD of the data obtained in duplicate wells in three experiments (**$p < 0.01$ *vs.* control). The deviation in each experiment was less than 10%.

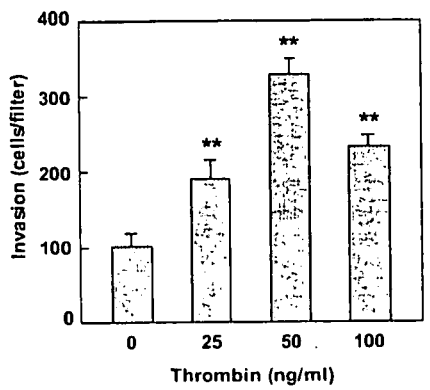

Fig. 2. **Dose dependency of the effect of thrombin on invasiveness.** MEM containing 1% FCS was used as the basal medium. The concentrations of thrombin indicated are the concentrations in the lower compartment. The data shown are means ± SD of data obtained in duplicate wells in three experiments (**$p < 0.01$ *vs.* control). The deviation in each experiment was less than 10%.

the dye was extracted in an end-over-end mixer with 600 μl of 50% ethanol in 50 mM sodium phosphate (pH 4.5) for 10 min, and absorbance was measured at 540 nm. The correlation between absorbance and cell number was confirmed in a preliminary experiment.

Chemotaxis Assay—Chemotaxis assays were performed with control inserts (Collaborative Biomedical Products, Bedford, MA, USA) in a similar manner to the invasion assay described above. The control inserts were not coated with Matrigel. MEM containing 1% FCS was used as the basal medium. The control inserts were pre-coated with fibronectin (5 μg/ml) as described for the pre-coating of the Matrigel invasion chamber in the thrombin-activity-depleted assay system.

Iodination of Thrombin and Determination of Binding—Thrombin was iodinated to a specific activity of 19.1 × 10^7 cpm/μg by the chloramine T method as described previously (*35–36*). After precoating 24-well plates with fibronectin (5 μg/ml) as described above, the cell suspen-

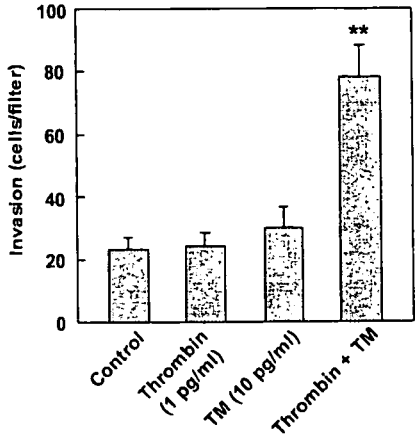

Fig. 3. **Effect of TM and thrombin on invasiveness in the thrombin-activity-depleted assay system.** Cells on which thrombin activity was depleted were used in the experiment. MEM containing 0.1% BSA was used as the basal medium. The data shown are means ± SD of data obtained in duplicate wells in three experiments (**$p < 0.01$ *vs.* control). The deviation in each experiment was less than 10%.

sions (1.22 × 10^5 cells in 0.45 ml of MEM) were seeded into each well and incubated in a humidified chamber at 37°C under 5% CO_2 for 2 h. The cells were then washed with 0.4 ml of MEM containing 15 mM Hepes (pH 7.2) and 0.1% BSA and incubated for 1.5 h at 37°C in the same buffer with various concentrations of [^{125}I]-thrombin in the presence or absence of a 100-fold excess amount of unlabeled thrombin. After washing the cells four times with the same ice-cold buffer, the cells were solubilized with 0.4 ml of 1 N NaOH for 1 h at 37°C. Specific binding was calculated as the difference between total binding and nonspecific binding.

RESULTS

Effect of TM on Invasiveness—Figure 1 shows the effects of TM on the invasive activity of MMT cells in the presence of 1% FCS. TM significantly stimulated invasive activity in a dose-dependent manner, resulting in an approximately 3-fold stimulation at 1–10 pg/ml. Figure 2 shows the effects of thrombin used as a positive control. Thrombin also stimulated invasive activity in a dose-dependent manner.

On the basis of these findings, we investigated the possibility that the stimulation of invasion by TM might be dependent on thrombin that may have been introduced into the assay system as described below. First, thrombin activity in the assay system was measured. The thrombin concentrations in freshly prepared 10% FCS and CS measured by the thrombin activity assay were 200 pg/ml and 2.8 ng/ml, respectively. The amount of thrombin on the cells measured in a similar manner was 35 pg/10^6 cells. Based on these values, the thrombin concentrations in the assay system with or without 1% FCS were estimated to be 24.48 and 4.48 pg/ml, respectively. Second, the action of TM was examined in the thrombin-activity-depleted assay system described in "MATERIALS AND METHODS," and depletion of thrombin activity in the

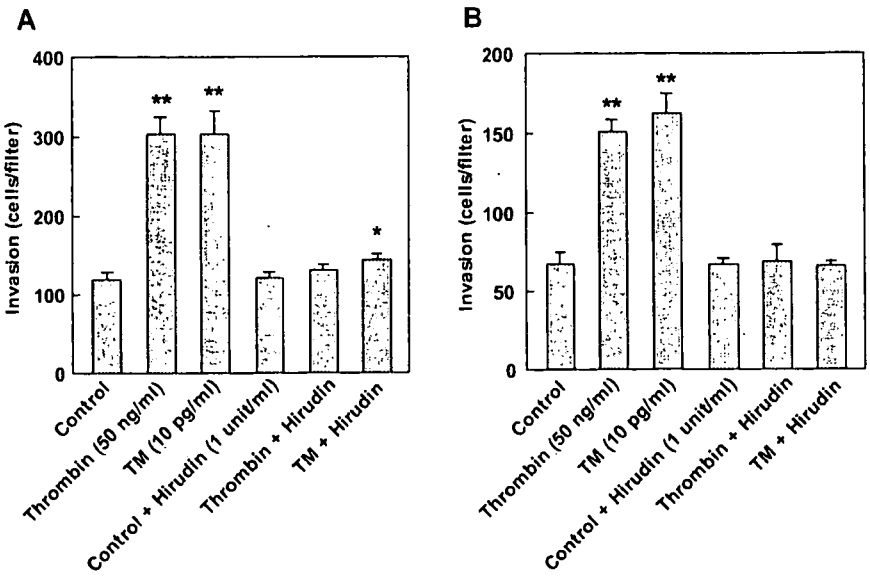

Fig. 4. **Effect of hirudin on the stimulation of invasion by TM.** (A) MEM containing 1% FCS was used as the basal medium. The indicated concentration of each factor is that in the lower compartment. The data shown are means ± SD of data obtained in duplicate wells in three experiments (*$p < 0.05$ *vs.* control; **$p < 0.01$ *vs.* control) (B) MEM containing 0.1% BSA was used as the basal medium. The data shown are means ± SD of data obtained in duplicate wells in three experiments (**$p < 0.01$ *vs.* control). The deviation in each experiment was less than 10%.

assay system was confirmed by the absence of any detectable thrombin activity on the cells. Figure 3 shows the effects of thrombin (1 pg/ml) and TM (10 pg/ml) on the invasive activity of cells in the thrombin-activity-depleted assay system. While neither thrombin or TM had any effect on invasion, TM plus thrombin stimulated invasion by approximately 3-fold.

Effect of Hirudin on the Stimulation of Invasion by TM—The action of TM was also examined in the presence of the specific thrombin inhibitor hirudin to investigate the possibility described above. Fig. 4, A and B, shows the effects of hirudin on the invasion-stimulating activity of TM in the presence and absence of 1% FCS. We used a 1 unit/ml concentration of hirudin in this experiment, because 50 ng/ml thrombin corresponds to 0.057 unit/ml, and so 1 unit/ml hirudin seemed adequate to inhibit this concentration of thrombin. As expected, hirudin (1 unit/ml) not only inhibited the stimulation by thrombin to control levels, but the stimulation by TM as well.

Effect of TM on Proliferation—Since tumor cell invasion consists of a series of events, including adhesion to the extracellular matrix (ECM) and chemotaxis, we investigated the effects of TM on these two events to clarify the molecular mechanism of the stimulation of invasive activity by TM. Before investigating the effect of TM on these processes, we investigated its effects on cell proliferation to confirm that the stimulation of invasive activity by TM is not an artifact of the enhancement of cell proliferation.

Figure 5 shows the effects of TM on MMT cell proliferation in the presence of 1% FCS. The numbers of cells in the presence of TM or thrombin did not differ from the numbers in the control cultures.

Effect of TM on Adhesion to Fibronectin—Figure 6 shows the effects of TM on adhesion to fibronectin, a basal lam-

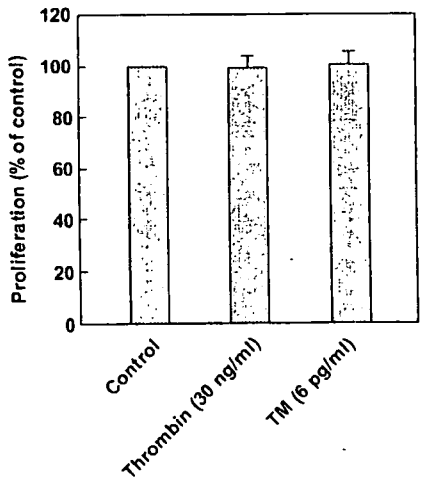

Fig. 5. **Effect of TM on proliferation.** MEM containing 1% FCS was used as the basal medium. The data shown are means ± SD of data obtained in duplicate dishes in three experiments. The deviation in each experiment was less than 10%.

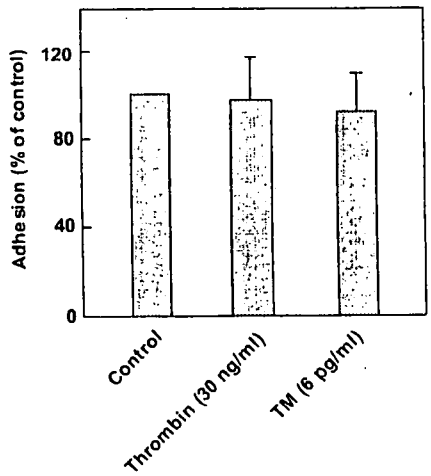

Fig. 6. **Effect of TM on adhesion to fibronectin.** MEM containing 1% FCS was used as the basal medium. The data shown are means ± SD of data obtained in duplicate wells in three experiments. The deviation in each experiment was less than 10%.

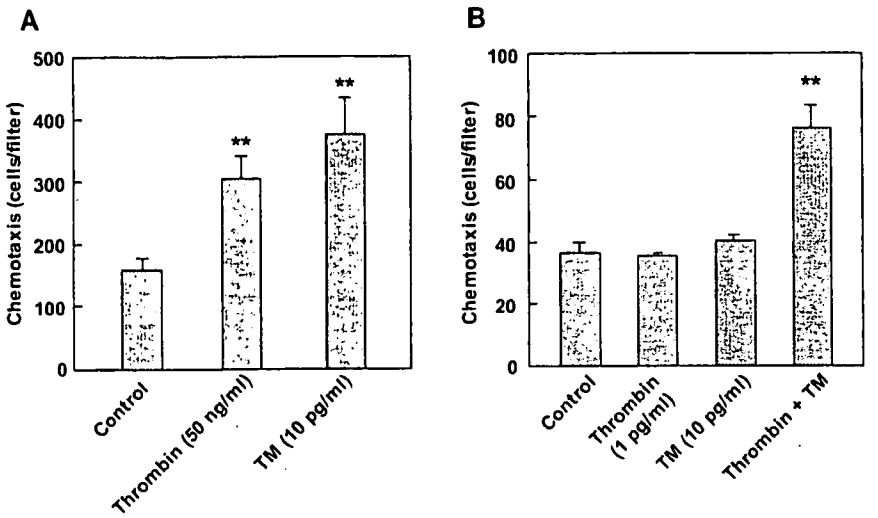

Fig. 7. **Effect of TM on chemotaxis.** (A) MEM containing 1% FCS was used as the basal medium. The data shown are means ± SD of data obtained in duplicate wells in three experiments (**$p < 0.01$ *vs.* control). (B) Cells on which thrombin activity was depleted were used in the experiment. MEM containing 0.1% BSA was used as the basal medium. The data shown are means ± SD of data obtained in duplicate wells in three experiments (**$p < 0.01$ *vs.* control). The deviation in each experiment was less than 10%.

ina component. Neither TM nor thrombin affected adhesion to fibronectin.

Effect of TM on Chemotaxis—Figure 7 (A and B), shows the effects of TM on chemotaxis by MMT cells in the presence of 1% FCS and in the thrombin-activity-depleted assay system, respectively. Both TM (10 pg/ml) and thrombin (50 ng/ml) significantly stimulated chemotaxis by MMT cells by approximately 1.9–2.3-fold in the former system, but neither TM (10 pg/ml) nor thrombin (1 pg/ml) affected chemotaxis in the latter system; TM plus thrombin, on the other hand, stimulated chemotaxis by approximately 2-fold.

Binding of Thrombin—Figure 8 shows the binding curves for specific [^{125}I]-thrombin binding sites on cells in the presence and absence of TM (10 pg/ml). These binding curves show the specific [^{125}I]-thrombin binding to be saturable at approximately 40 ng/ml, and that TM has no effect on the specific binding of [^{125}I]-thrombin. A similar binding experiment was performed in the [^{125}I]-thrombin concentration range of 1–10 pg/ml, but no specific binding was detected independent of the presence or absence of TM, probably because the absolute amount of radioactivity used was too low to be detected as specific binding.

DISCUSSION

In the present study, we show that, at its maximum effective dose, TM stimulates the invasive activity of MMT cells *in vitro* by approximately 3-fold. As far as we know, this is the first time that TM has been shown to stimulate the invasive activity of tumor cells *in vitro*. Similarly, exogenous thrombin causes maximal stimulation of invasion at 50 ng/ml, which is a concentration more than 1,000-fold higher than the maximum effective dose of TM.

Since TM acts as a cofactor for the thrombin-catalyzed activation of protein C and increases the rate of the reaction by >1,000-fold (*8*), the stimulation by TM may have been due to TM interacting with thrombin, which had been introduced into the assay system, and acting as a cofactor for thrombin-stimulated invasion of MMT cells, thus lowering the effective concentration of thrombin. This possibility seems to be supported by the detection of thrombin activity in the assay systems, the requirement for thrombin for stimulation by TM in the thrombin-activity-depleted assay system, and the inhibition of stimulation by hirudin. It is noteworthy that the thrombin concentration required for stimulation by TM in the thrombin-activity-depleted assay system is more than 20,000-fold less than the concentration required for thrombin to stimulate invasion. On the other hand, the control level was not inhibited by hirudin in the presence of 1% FCS, probably due to the lower thrombin concentration in the assay system compared with the effective concentration of exogenous thrombin.

There have been two studies examining the effect of TM on the invasive activity of tumor cells. Matsushita *et al.* showed that a subcloned human esophageal squamous cell carcinoma line with low TM expression is more invasive than a high TM-expressing clone (*37*). In their study, the action of TM does not seem to be due to an acceleration of its thrombin cofactor activity, because the difference between the cell lines with low and high TM expression with respect to their cofactor activity for protein C activation by thrombin was less than 13% and significantly lower than their TM levels and invasive activities. Hosaka *et al.* showed that TM (10–100 ng/ml)

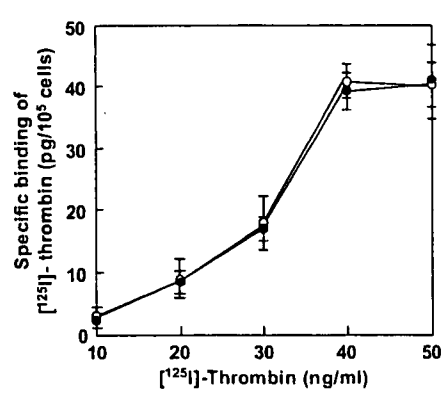

Fig. 8. **Binding of [^{125}I]-thrombin.** Specific binding of [^{125}I]-thrombin to cells in the absence (solid circles) and presence of TM (10 pg/ml) (open circles) was measured. The data shown are representative specific binding curves for [^{125}I]-thrombin binding sites and are means ± SD of data obtained in triplicate wells.

inhibits the invasive activity of mouse melanoma cells *in vitro* (*38*), and TM has also been found to decrease the proliferation of tumor cell lines subcloned from patients with malignant melanomas (*39*). None of these inhibitory effects were inhibited by hirudin.

In contrast to these studies, the present study shows that TM enhances the invasive activity of MMT cells and indicates that the action of TM is entirely dependent on thrombin as described above. Therefore, the mode and mechanism of action of TM in MMT cells seems to be different from its mode and mechanism of action in the squamous cell carcinoma line and melanoma cells.

It is useful to speculate on the role of TM in tumorigenesis based on the findings of our study, because tumor cell invasion through the basement membrane is a critical step in the process of metastasis (*29–30*). Several studies have shown that TM levels in serum increase in patients with certain tumors (*26–28*), as described in the Introduction. Thus, the results of this study suggest that the soluble form of TM may play a positive role in the malignancy of some kinds of tumors, probably by enhancing the metastatic potential of thrombin. On the other hand, TM on the cell surface may act as a negative regulator to thrombin, because thrombin is degraded as the thrombin-TM complex by its internalization after binding to TM on the cell surface (*40*). This possibility may be supported by the findings that the expression level of TM is negatively correlated with the malignancy of some carcinomas (*23–25*), as described in the Introduction.

Tumor cell invasion is a complex process that involves adhesion to ECM, degradation of ECM, and chemotaxis (*41*). Chemotaxis is the essential step in invasion as reviewed by Wells (*42*). The results of the present study show that both TM and thrombin stimulate chemotaxis in the presence of 1% FCS, and that TM plus thrombin stimulate chemotaxis in the thrombin-activity-depleted assay system. Both of these findings are consistent with previous reports that thrombin stimulates chemotaxis (*17*, *18*), and the presence of specific binding sites for thrombin on cells indicates that these actions are mediated by thrombin receptors.

However, other actions of thrombin may also be involved in the stimulation of tumor cell invasion, because the enhancement of chemotaxis alone is insufficient to account for the increase in tumor cell invasion. One such other possible action of thrombin is the stimulation of the matrix metalloprotease (MMP)–mediated degradation of a variety of ECM proteins, including collagens type IV, V, VII, and X, fibronectin, laminin (*43–47*), elastin (*48–49*), proteoglycans (*49–51*), and entactin (*52*). Several reports have indicated that thrombin increases the active forms of MMP-2 and MMP-9 (*53–59*), and plays important roles in the enhancement of tumor cell invasion and metastasis (*34*, *60–68*). There are also reports that thrombin stimulates the release of MMP-2 (*69*), the expression of MMP-1 and MMP-3 (*70*), and the expression of MMP-9 mRNA (*71*). Another possible action is the stimulation of MMP-independent degradation of ECM. This possibility appears to be supported by the finding that thrombin stimulates the expression of urokinase-type plasminogen activator, a factor involved in the degradation of ECM protein (*72*), and stimulates the heparinase-mediated release of heparan sulfate from ECM (*73*).

In conclusion, the results of this study show that TM stimulates the invasive activity of MMT cells, probably by acting as a cofactor for the thrombin-stimulated invasion of cells mediated by thrombin receptors, and by lowering the effective concentration of thrombin. Further, the results indicate that the stimulation is mainly caused by an enhancement of chemotaxis.

This study was supported, in part, by a Grant-in-Aid for research on health sciences focusing on drug innovation from the Japan Health Sciences Foundation.

REFERENCES

1. Esmon, C.T. and Owen, W.G. (1981) Identification of an endothelial cell cofactor for thrombin-catalyzed activation of protein C. *Proc. Natl Acad. Sci. USA* **78**, 2249–2252
2. Esmon, C.T. (1989) The roles of protein C and thrombomodulin in the regulation of blood coagulation. *J. Biol. Chem.* **264**, 4743–4746
3. Ishii, H. and Majerus, P.W. (1985) Thrombomodulin is present in human plasma and urine. *J. Clin. Invest.* **76**, 2178–2181
4. Molinari, A., Giorgetti, C., Lansen, J., Vaghi, F., Orsini, G., Faioni, E.M., and Mannucci, P.M. (1992) Thrombomodulin is a cofactor for thrombin degradation of recombinant single-chain urokinase plasminogen activator "in vitro" and in a perfused rabbit heart model. *Thromb. Haemost.* **67**, 226–232
5. Bajzar, L., Morser, J., and Nesheim, M. (1996) TAFI, or plasma procarboxypeptidase B, couples the coagulation and fibrinolytic cascades through the thrombin-thrombomodulin complex. *J. Biol. Chem.* **271**, 16603–16608
6. Pekovich, S.R., Bock, P.E., and Hoover, R.L. (2001) Thrombin-thrombomodulin activation of protein C facilitates the activation of progelatinase A. *FEBS Lett.* **494**, 129–132
7. Esmon, N.L., Carroll, R.C., and Esmon, C.T. (1986) Thrombomodulin blocks the ability of thrombin to activate platelets. *J. Biol. Chem.* **258**, 12238–12242
8. Esmon, C.T., Esmon, N.L., and Harris, K.W. (1983) Complex formation between thrombin and thrombomodulin inhibits both thrombin-catalyzed fibrin formation and factor V activation. *J. Biol. Chem.* **257**, 7944–7947
9. Parkinson, J.F., Bang, N.U., and Garcia, J.G. (1993) Recombinant human thrombomodulin attenuates human endothelial cell activation by human thrombin. *Arterioscler. Thromb.* **13**, 1119–1123
10. Li, J., Garnette, C.S., Cahn, M., Claytor, R.B., Rohrer, M.J., Dobson, J.G. Jr., Gerlitz. B., and Cutler, B.S. (2000) Recombinant thrombomodulin inhibits arterial smooth muscle cell proliferation induced by thrombin. *J. Vasc. Surg.* **32**, 804–813
11. Lafay, M., Laguna, R., Le Bonniec, B.F., Lasne, D., Aiach, M., and Rendu, F. (1998) Thrombomodulin modulates the mitogenic response to thrombin of human umbilical vein endothelial cells. *Thromb. Haemost.* **79**, 848–852
12. Nierodzik, M.L., Plotkin, A., Kajumo, F., and Karpatkin, S. (1991) Thrombin stimulates tumor-platelet adhesion *in vitro* and metastasis *in vivo*. *J. Clin. Invest.* **87**, 229–236
13. Nierodzik, M.L., Kajumo, F., and Karpatkin, S. (1992) Effect of thrombin treatment of tumor cells on adhesion of tumor cells to platelets *in vitro* and tumor metastasis *in vivo*. *Cancer Res.* **52**, 3267–3272
14. Esumi, N., Fan, D., and Fidler, J.I. (1991) Inhibition of murine melanoma experimental metastasis by recombinant desulfatohirudin, a highly specific thrombin inhibitor. *Cancer Res.* **51**, 4549–4556
15. Wojtukiewicz, M.Z., Tang, D.G., Ben-Josef, E., Renaud, C., Walz, D.A., and Honn, K.V. (1995) Solid tumor cells express functional 'tethered ligand' thrombin receptor. *Cancer Res.* **55**, 698–704
16. Even-Ram, S., Uziely. B., Cohen, P., Grisaru-Granovsky, S., Maoz, M., Ginzburg, Y., Reich, R., Vlodavsky, I., and Bar-

Shavit, R. (1998) Thrombin receptor overexpression in malignant and physiological invasion processes. *Nat. Med.* **4**, 909–914
17. Hernandez-Rodriguez, N.A., Correa, E., Contreras-Paredes, A., and Green, L. (1999) Evidence that thrombin present in lungs of patients with pulmonary metastasis may contribute to the development of the disease. *Lung Cancer* **26**, 157–167
18. Henrikson, K.P., Salazar, S.L., Fenton, J.W. II., and Pentecost, B.T. (1999) Role of thrombin receptor in breast cancer invasiveness. *Br. J. Cancer* **79**, 401–406
19. Ogawa, H., Yonezawa, S., Maruyama, I., Matsushita, Y., Tezuka, Y., Toyoyama, H., Yanagi, M., Matsumoto, H., Nishijima, H., Shimotakahara, T., Aikou, T., and Sato, E. (2000) Expression of thrombomodulin in squamous cell carcinoma of the lungs: its relationship to lymph node metastasis and prognosis of the patients. *Cancer Lett.* **149**, 95–103
20. Takebayashi, Y., Yamada, K., Maruyama, I., Fujii, R., Akiyama, S., and Aikou, T. (1995) The expression of thymidine phosphorylase and thrombomodulin in human colorectal carcinomas. *Cancer Lett.* **92**, 1–7
21. Ordonez, N.G. (1997) Value of thrombomodulin immunostaining in the diagnosis of transitional cell carcinoma: a comparative study with carcinoembryonic antigen. *Histopathology* **31**, 517–524
22. Ordonez, N.G. (1998) Thrombomodulin expression in transitional cell carcinoma. *Am. J. Clin. Pathol.* **110**, 385–390
23. Matsumoto, M., Natsugoe, S., Nakashima, S., Shimada, M., Nakano, S., Kusano, C., Baba, M., Takao, S., Matsushita, Y., and Aikou, T. (2000) Biological evaluation of undifferentiated carcinoma of the esophagus. *Ann. Surg. Oncol.* **7**, 204–209
24. Suehiro, T., Shimada, M., Matsumata, T., Taketomi, A., Yamamoto, K., and Sugimachi, K. (1995) Thrombomodulin inhibits intrahepatic spread in human hepatocellular carcinoma. *Hepatology* **21**, 1285–1290
25. Wilhelm, S., Schmitt, M., Parkinson, J., Kuhn, W., Graeff, H., and Wilhelm O.G. (1998) Thrombomodulin, a receptor for the serine protease thrombin, is decreased in primary tumors and metastases but increased in ascitic fluids of patients with advanced ovarian cancer FIGO IIIc. *Int. J. Oncol.* **13**, 645–651
26. Lindahl, A.K., Boffa, M.C., and Abildgaard, U. (1993) Increased plasma thrombomodulin in cancer patients. *Thromb. Haemost.* **69**, 112–114
27. Boffa, M.C., Lapeyrere, C., Berard, M., Lindahl, A.K., Flageul, B., Chemaly, P., Abildgaard, U., and Dubertret, L. (1994) Plasma thrombomodulin level in malignancy varies according to the tumor type. *Nouv. Rev. Fr. Hematol.* **36**, S87–88
28. Salmaggi, A., Eoli, M., Frigerio, S., Ciusani, E., Silvani, A., and Boiardi, A. (1999) Circulating intercellular adhesion molecule-1 (ICAM-1), vascular cell adhesion molecule-1 (VCAM-1) and plasma thrombomodulin levels in glioblastoma patients. *Cancer Lett.* **146**, 169–172
29. Liotta, L.A. (1986) Tumor invasion and metastases-role of the extracellular matrix: Rhoads Memorial Award lecture. *Cancer Res.* **46**, 1–7
30. Terranova, V.P., Hujanen, E.S., and Martin, G.R. (1986) Basement membrane and the invasive activity of metastatic tumor cells. *J. Natl Cancer Inst.* **77**, 311–316
31. Gomi, K., Zushi, M., Honda, G., Kawahara, S., Matsuzaki, O., Jr., Kanabayashi, T., Yamamoto, S., Maruyama, I., and Suzuki, K. (1990) Antithrombotic effect of recombinant human thrombomodulin on thrombin-induced thromboembolism in mice. *Blood* **75**, 1396–1399
32. Niimi, S., Oshizawa, T., Naotsuka, M., Ohba, S., Yokozawa, A., Murata, T., and Hayakawa, T. (2002) Establishment of a standard assay method for human thrombomodulin and determination of the activity of the Japanese reference standard. *Biologicals* **30**, 69–76
33. Kawabata, S., Miura, T., Morita, T., Kato, H., Fujikawa, K., Iwanaga, S., Takada, K., Kimura, T., and Sakakibara, S. (1988) Highly sensitive peptide-4-methylcoumaryl-7-amide substrates for blood-clotting proteases and trypsin. *Eur. J. Biochem.* **172**, 17–25
34. Deryugina, E.I., Luo, G.X., Reisfeld, R.A., Bourdon, M.A., and Strongin, A. (1997) Tumor cell invasion through matrigel is regulated by activated matrix metalloproteinase-2. *Anticancer Res.* **17**, 3201–3210
35. Greenwood, F.C., Hunter, W.M., Glover, J.S. (1963) The preparation of ^{131}I-labelled human growth hormone of high specific radioactivity. *Biochem. J.* **89**, 114–123
36. Haeuptle, M.T., Aubert, M.L., Djiane J., Kraehenbuhl, J.P. (1983) Binding sites for lactogenic and somatogenic hormones from rabbit mammary gland and liver. *J. Biol. Chem.* **258**, 305–314
37. Matsushita, Y., Yoshiie, K., Imamura, Y., Ogawa, H., Imamura, H., Takao, S., Yonezawa, S., Aikou, T., Maruyama, I., and Sato, E. (1998) A subcloned human esophageal squamous cell carcinoma cell line with low thrombomodulin expression showed increased invasiveness compared with a high thrombomodulin-expressing clone—thrombomodulin as a possible candidate for an adhesion molecule of squamous cell carcinoma. *Cancer Lett.* **127**, 195–201
38. Hosaka, Y., Higuchi, T., Tsumagari, M., and Ishii, H. (2000) Inhibition of invasion and experimental metastasis of murine melanoma cells by human soluble thrombomodulin. *Cancer Lett.* **161**, 231–240
39. Zhang, Y., Weiler-Guettler, H., Chen, J., Wilhelm, O., Deng, Y., Qiu, F., Nakagawa, K., Klevesath, M., Wilhelm, S., Bohrer, H., Nakagawa, M., Graeff, H., Martin, E., Stern, D.M., Rosenberg, R.D., Ziegler, R., and Nawroth, P.P. (1998) Thrombomodulin modulates growth of tumor cells independent of its anticoagulant activity. *J. Clin. Invest.* **101**, 1301–1309
40. Maruyama, I. and Majerus, P.W. (1985) The turnover of thrombin-thrombomodulin complex in cultured human umbilical vein endothelial cells and A549 lung cancer cells. Endocytosis and degradation of thrombin. *J. Biol. Chem.* **260**, 15432–15438
41. Hart, I.R., Goode, N.T., and Wilson, R.E. (1989) Molecular aspects of the metastatic cascade. *Biochim. Biophys. Acta* **989**, 65–84
42. Wells, A. (2000) Tumor invasion: role of growth factor-induced cell motility. *Adv. Cancer Res.* **78**, 31–101
43. Matrisian, L.M. (1990) Metalloproteinases and their inhibitors in matrix remodeling. *Ternds Genet.* **6**, 121–125
44. Collier, I.E., Wilhelm, S.M., Eisen, A.Z., Marmer, B.L., Grant. G.A., Seltzer. J.L., Kronberger, A., He. C.S., Bauer, E.A., and Goldberg, G.I. (1988) H-ras oncogene-transformed human bronchial epithelial cells (TBE-1) secrete a single metalloprotease capable of degrading basement membrane collagen. *J. Biol. Chem.* **263**, 6579–6587
45. Wilhelm, S.M., Collier, I.E., Marmer, B.L., Eisen, A.Z., Grant, G.A., and Goldberg, G.I. (1989) SV40-transformed human lung fibroblasts secrete a 92-kDa type IV collagenase which is identical to that secreted by normal human macrophages. *J. Biol. Chem.* **264**, 17213–17221
46. Fessler, L.I., Duncan, K.G., Fessler, J.H., Salo, T., and Tryggvason, K. (1984) Identification of the procollagen IV cleavage products produced by a specific tumor collagenase. *J. Biol. Chem.* **259**, 9783–9789
47. Woessner, J.F. Jr. (1991) Matrix metalloproteinases and their inhibitors in connective tissue remodeling. *FASEB J.* **5**, 2145–2154
48. Senior, R.M., Griffin, G.L., Fliszar, C.J., Shapiro, S.D., Goldberg, G.I., and Welgus, H.G. (1991) Human 92- and 72-kilodalton type IV collagenases are elastases. *J. Biol. Chem.* **266**, 7870–7875
49. Murphy, G., Cockett, M.I., Ward, R.V., and Docherty, A.J. (1991) Matrix metalloproteinase degradation of elastin, type IV collagen and proteoglycan. A quantitive comparison of the activities of 95 kDa and 72 kDa gelatinases, stromelysins-1 and -2 and punctuated metalloproteinae (PUMP). *Biochem. J.* **277**, 277–279
50. Nguyen, Q., Murphy, G., Hughes, C.E., Mort, J.S., and Roughley, P.J. (1993) Matrix metalloproteinases cleave at two distinct sites on human cartilage link protein. *Biochem. J.* **295**, 595–598

51. Fosang, A.J., Last, K., Knauper, V., Neame, P.J., Murphy, G., Hardingham, T.E., Tschesche, H., and Hamilton, J.A. (1993) Fibroblast and neutrophil collagenases cleave at two sites in the cartilage aggrecan interglobular domain. *Biochem. J.* **295**, 273–276
52. Sires, U.I., Griffin, G.L., Broekelmann, T.J., Mecham, R.P., Murphy, G., Chung, A.E., Welgus, H.G., and Senior, R.M. (1993) Degradation of entactin by matrix metalloproteinases. Susceptibility to matrilysin and identification of cleavage sites. *J. Biol. Chem.* **268**, 2069–2074
53. Zucker, S., Conner, C., DiMassmo, B.I., Ende, H., Drews, M., Seiki, M., and Bahou, W.F. (1995) Thrombin induces the activation of progelatinase A in vascular endothelial cells. Physiologic regulation of angiogenesis. *J. Biol. Chem.* **270**, 23730–23738
54. Galis, Z.S., Kranzhofer, R., Fenton, J.W. II., and Libby, P. (1997) Thrombin promotes activation of matrix metalloproteinase-2 produced by cultured vascular smooth muscle cells. *Arterioscler. Thromb. Vasc. Biol.* **17**, 483–489
55. Nguyen, M., Arkell, J., and Jackson, C.J. (1999) Thrombin rapidly and efficiently activates gelatinase A in human microvascular endothelial cells via a mechanism independent of active MT1 matrix metalloproteinase. *Lab. Invest.* **79**, 467–475
56. Pekovich, S.R., Bock, P.E., and Hoover, R.L. (2001) Thrombin-thrombomodulin activation of protein C facilitates the activation of progelatinase A. *FEBS Lett.* **694**, 129–132
57. Lafleur, M.A., Hollenberg, M.D., Atkinson. S.J., Knauper, V., Murphy, G., and Edwards, D.R. (2001) Activation of pro-(matrix metalloproteinase-2) (pro-MMP-2) by thrombin is membrane-type-MMP-dependent in human umbilical vein endothelial cells and generates a distinct 63 kDa active species. *Biochem. J.* **357**, 107–115
58. Maragoudakis, M.E., Kraniti, N., Giannopoulou, E., Alexopoulos, K., and Matsuokas, J. (2001) Modulation of angiogenesis and progelatinase A by thrombin receptor mimetics and antagonists. *Endothelium* **8**, 195–205
59. Liu, Y., Gilcrease, M.Z., Henderson, Y., Yuan, X.H., Clayman, G.L., and Chen, Z. (2001) Expression of protease-activated receptor 1 in oral squamous cell carcinoma. *Cancer Lett.* **169**, 173–180
60. Stetler-Stevenson, W.G., Aznavoorian, S., and Liotta, L.A. (1993) Tumor cell interactions with the extracellular matrix during invasion and metastasis. *Annu. Rev. Cell. Biol.* **9**, 541–573
61. Himelstein, B.P., Canete-Soler, R., Bernhard, E.J., Dilks, D.W., and Muschel, R.J. (1994) Metalloproteinases in tumor progression: the contribution of MMP-9. *Invasion Metastasis.* **14**, 246–258
62. Bernhard, E.J., Gruber, S.B., and Muschel, R.J. (1994) Direct evidence linking expression of matrix metalloproteinase 9 (92-kDa gelatinase/collagenase) to the metastatic phenotype in transformed rat embryo cells. *Proc. Natl Acad. Sci. USA* **91**, 4293–4297
63. MacDougall, J.R., and Matrisian. L.M. (1995) Contribution of tumor and stromal matrix metalloroteinases to tumor progression, invasion and metastasis. *Cancer Metastasis Rev.* **14**, 351–362
64. Hua, J. and Muschel, R.J. (1996) Inhibition of matrix metalloproteinase 9 expression by a ribozyme blocks metastasis in a rat sarcoma model system. *Cancer Res.* **56**, 5279–5284
65. Kim, J., Yu, W., Kovalski, K., and Ossowski, L. (1998) Requirement for specific proteases in cancer cell intravasation as revealed by a novel semiquantitative PCR-based assay. *Cell* **94**, 353–362
66. Hahn-Dantona, E., Ramos-DeSimone, N., Sipley, J., Nagase, H., French, D.L., and Quigley, J.P. (1999) Activation of proMMP-9 by a plasmin/MMP-3 cascade in a tumor cell model. Regulation by tissue inhibitors of metalloproteinases. *Ann. N. Y. Acad. Sci.* **878**, 372–387
67. John, A. and Tuszynski, G. (2001) The role of matrix metalloproteinases in tumor angiogenesis and tumor metastasis. *Pathol. Oncol. Res.* **7**, 14–23
68. Giannelli, G. and Antonaci, S. (2002) Gelatinases and their inhibitors in tumor metastasis: from biological research to medical applications. *Histol. Histopathol.* **17**, 339–345
69. Fernandez-Patron, C., Zhang, Y., Radomski, M.W., Hollenberg, M.D., and Davidge, S.T. (1999) Rapid release of matrix metalloproteinase (MMP)-2 by thrombin in the rat aorta: modulation by protein tyrosine kinase/phosphatase. *Thromb. Haemost.* **82**, 1353–1357
70. Duhamel-Clérin, E., Orvain, C., Lanza, F., Cazenave, J.P., and Klein-Soyer, C. (1997) Thrombin receptor-mediated increase of two matrix metalloproteinases, MMP-1 and MMP-3, in human endothelial cells. *Arterioscler. Thromb. Vasc. Biol.* **17**, 1931–1938
71. Liu, W.H., Chen, X.M., and Fu, B. (2000) Thrombin stimulates MMP-9 mRNA expression through AP-1 pathway in human mesangial cells. *Acta. Pharmacol. Sin.* **21**, 641–645
72. Yoshida, E., Verrusio, E.N., Mihara, H., Oh, D., and Kwaan, H.C. (1994) Enhancement of the expression of urokinase-type plasminogen activator from PC-3 human prostate cancer cells by thrombin. *Cancer Res.* **54**, 3300–3304
73. Benezra, M., Vlodavsky, I., and Bar-Shavit, R. (1992) Thrombin enhances degradation of heparan sulfate in the extracellular matrix by tumor cell heparanase. *Exp. Cell Res.* **201**, 208–215

日薬理誌 126, 433 (2005)

バイオロジクスのトランスレーショナルリサーチ（その1）

最近医薬品を含めた医療技術開発におけるトランスレーショナルリサーチ（TR）の重要性が叫ばれ，様々な学会等でトピックとして取り上げられている．我が国の医薬品開発環境の最も大きな問題点の一つは，臨床研究環境の未整備であることは衆目の一致するところであるが，取り上げられる機会が多い割には，TRの要点についての理解は必ずしも深まってはいないように思われる．そこで本稿ではバイオロジクス，特に筆者の専門とするバイオテクノロジー応用医薬品（バイオ医薬品）の開発を目指してTRを実施する上で考慮すべき点を，規制ガイドラインを参考に，2回に分けて考えてみる．

TRの本来の意味は，「探索的臨床研究＝基礎的研究成果を臨床へ導入するための臨床開発の初期段階のプロセス」であるが，今現在本来の意味のTRを行う上での条件等を定めた公的なガイドラインはない．しかしTRの対象を治験レベルまで広げると，その実施の条件，および注意点は既存の各種ガイドライン等から浮かび上がる．

バイオ医薬品の中で既に最も実用化が実現している医薬品は，遺伝子組換え技術や細胞培養技術を用いて製造されたタンパク質性医薬品（エリスロポエチン，インスリン類，成長ホルモン，インターフェロン，ヒトモノクローナル抗体等）であるが，我が国においてこれら医薬品開発にあたってまず参照すべきガイドラインは，(1)薬審第243号通知（昭和59年3月30日）「組換えDNA技術応用医薬品ガイドライン」；(2)薬審1第10号通知（昭和63年6月6日）「細胞培養技術応用医薬品ガイドライン」；(3)都道府県衛生主管部(局)薬務主管課宛事務連絡（平成元年5月）「薬審1第10号通知に関する質疑応答」である．しかしその後，医薬品の開発段階で考慮することが必要な技術的要件に関するICH国際調和ガイドラインが作成され，国内ガイドラインとして公表されている．これらは企業による新薬開発を対象としたものであるが，生体内タンパク質の医薬品への応用をめざしたトランスジェニックリサーチの実施の条件を考える上での参考となる．以下がこれらのガイドラインである：(1)「遺伝子発現構成体ガイドライン（厚生省医薬安全局審査管理課長通知 医薬審第3号 平成10年1月6日）」：主として遺伝子組換え技術を用いて医薬品製造用細胞を作製する場合の遺伝子発現構成体の設計，作製，細胞への導入，導入後の安定性チェックに関する注意点；(2)「細胞基材ガイドライン（厚生省医薬安全局審査管理課長通知 医薬審第873号 平成12年7月14日」：バイオ医薬品の製造に使用する細胞基材の由来，調整，特性解析，管理に関する注意点；(3)「安定性ガイドライン（厚生省医薬安全局審査管理課長通知 医薬審第6号 平成10年1月6日）」：タンパク質性医薬品の安定性試験に関する注意点；(4)「ウィルス安全性ガイドライン（厚生省医薬安全局審査管理課長通知 医薬審第329号 平成12年2月22日）」：製品のウィルス汚染に関する配慮，試験に関する注意点；(5)「タンパク質性医薬品の特性解析・品質規格ガイドライン（厚生省医薬安全局審査管理課長通知 医薬審第571号 平成13年5月1日）」：医薬品の特性解析および品質規格設定にあたっての注意点；(6)「同等性・同質性ガイドライン（厚生労働省医薬食品局審査管理課長通知 薬食審発第0426001号 平成17年4月26日）」：製造工程の変更にともなう医薬品の同等性／同質性評価にあたっての注意点；(7)「非臨床安全性評価ガイドライン（厚生省医薬安全局審査管理課長通知 医薬審第326号 平成12年2月22日）」：臨床試験に先立つ非臨床安全性試験に関する注意点．

これらタンパク性医薬品を低分子化学合成医薬品と比較すると，(1)タンパク質の高次構造解析に限界があるため，構造の完全な同定，確認がしばしば困難であり，生物活性に基づく評価が重要；(2)製造の一定性を確保することが困難な細胞を利用して製造し，また翻訳後修飾等により分子多様性がある物質が多いので，物質の一定性の確保が重要；(3)常温で不安定な物質が多く，実時間での安定性の確認および保存条件の確保が重要；(4)製造に生体由来原料を使用するので，感染症に対する配慮が重要；(5)品質確保のために遺伝子発現構成体，細胞基材，宿主由来不純物など製造工程管理が重要；(6)物質としては天然のタンパク質に近いので，薬理作用および作用メカニズムの予測は容易であるが，種差により動物を用いた非臨床試験が不適切な場合もある；(7)体内動態試験は方法論に限界がある場合がある；(8)ヒトタンパク質の場合，種差，抗原性等により，げっ歯類動物を用いた非臨床安全性試験の予測性に限界がある，といった特徴がある．とりわけバイオロジクスの場合は被験物質の一定性の確保は，いかなるTRにおいてもデータの信頼性をはかる上で極めて重要であり，大学等での研究では見逃されがちな点である．（次号に続く）

国立医薬品食品衛生研究所 生物薬品部
川西 徹 Toru Kawanishi
e-mail: kawanish@nihs.go.jp

キーワード：トランスレーショナルリサーチ，
バイオロジクス，創薬

＊総　　説＊

医薬品研究
Pharm. Regul. Sci.
36(4)163～193(2005)

抗体医薬の現状と展望

新見　伸吾*，原島　　瑞*，川西　　徹*，早川　堯夫**

(受付：平成17年1月21日，受理：平成17年3月9日)

State and Perspective of Antibody Therapeutics

Shingo NIIMI*, Mizuho HARASHIMA*,
Toru KAWANISHI* and Takao HAYAKAWA**

はじめに

抗体医薬の始まりは19世紀終わりのエミール・ベーリングと北里柴三郎による血清療法にさかのぼる．彼等は加熱変性させたジフテリア菌毒素をウサギに注射することにより，ジフテリアに対する抵抗性を獲得させた．更に，そのウサギの血清を他のウサギに注射すると，ジフテリアに対する抵抗性をワクチンの接種されていないウサギに移せることを発見し，これをヒトに応用した[1]．その後，ヒト血液から精製したガンマーグロブリン製剤が開発され老人や術後の患者の日和見感染症，川崎病の自己免疫病に多用されている．

1975年にモノクローナル抗体作成技術がケラーとミルシュタインにより[2]開発されてから，対象となるターゲットに対して高親和性と特異性の高いマウスモノクローナル抗体については基礎研究だけでなく治療薬を目指した膨大な研究が行われてきた．実際，モノクローナル抗体治療薬は①分子化合物に比較して基本的に細胞毒性が低いかもしくは無い，②比較的長期にわたり血中濃度の維持が容易である，③結合対象となるリガンド選択性・特異性に優れている，④抗原の捕捉だけでなく生体内からの排除が可能であるといったメリットがある．しかしながら，マウスモノクローナル抗体の治療薬としての利用はヒトへの免疫原性により繰り返し投与時の効果の減弱，アナフィラキシーショックの危険性のために，非常に限られたものであった．そこで今日までに，免疫原性，アナフィラキシーショックの危険性を低減し，繰り返し投与を可能にするヒト型モノクローナル抗体を作成する様々な技術が生み出された．このようにして作成されたヒト型モノクローナル抗体の一部は医薬品として承認され臨床で用いられており，現在臨床応用を目指して開発中のものも多い(Table 1, Table 2)．そこで本稿においては抗体医薬の基礎と臨床応用，問題点等について概説する．

1．抗体医薬の作成

1.1　キメラ抗体，ヒト化抗体

キメラ抗体は遺伝子組換え技術を用いてマウスモノクローナル抗体の定常 constant (C) 領域をヒト抗体のC領域に置き換えたものである[3] (Fig. 1)．更にヒト化抗体は抗体タンパク質の三次元構造をもとに，抗原が実際に結合する相補性決定領域 complementarity determining region (CDR) の1から3を残して，それ以外の部分であるフレーム領域

＊ 国立医薬品食品衛生研究所生物薬品部　東京都世田谷区上用賀1-18-1 (〒158-8501)
Division of Biological Chemistry and Biologocals, National Institute of Health Sciences, 1-18-1 Kamiyoga, Setagaya-ku, Tokyo 158-8501, Japan
＊＊ 国立医薬品食品衛生研究所　東京都世田谷区上用賀1-18-1 (〒158-8501)
National Institute of Health Sciences, 1-18-1 Kamiyoga, Setagaya-ku, Tokyo 158-8501, Japan

Table 1 認可された抗体医薬

商品名 (抗体名)	企業	日本での 販売元	タイプ (抗原)	適応症	認可 (年)
Repro® (*Abciximab*)	Centocor社/ Eli Lilly社	全薬工業（株）	キメラ (gp II b III a)	PTCA後再狭窄	1994
Rituxan® (*Rituximab*)	IDEC社/Roche 社/Genentech社		キメラ (CD20)	ノンホジキン リンホーマ	1997
Zenepax® (*Daclizumab*)	Roche社		ヒト化 (IL-2R)	腎移植	1997
Remicade® (*Avakine*)	Centocor社		キメラ (TNF-α)	クローン病 慢性関節リウマチ	1998
Synagis® (*Palibizumab*)	MedImmune社/ Abott社		ヒト化 (RSV)	RSV小児感染	1998
Simulect® (*Basilicimab*)	Novartis社		ヒト化 (IL-2)	腎移植	1998
Herceptin® (*Trastuzumab*)	Genentech社/ Roche社	日本ロシュ（株）	ヒト化 (HER2)	乳癌	1998
Mylotarg® (*Gemtuzumab*)	Cellutech社/ AHP社		抗癌剤－コンジュゲート (CD33)	急性骨髄性白血病	2000
Zevalin® (*Iritumomab*)	IDEC社/ Schering AG社		^{90}Y-コンジュゲート (CD20)	ノンホジキン リンホーマ	2002
Bexxar® (*Tositumomab*)	Coulter社/ SKB社		^{131}I-コンジュゲート (CD20)	ノンホジキン リンホーマ	2002

（文献 122 より許可を得て転載）

Table 2 開発中の抗体医薬

段階	数					
	合計	キメラ抗体	ヒト化抗体	完全ヒト抗体	マウス抗体	その他
発売中	11	4	5	0	2	0
申請中	3	0	1	1	1	0
フェーズIII	20	1	9	2	8	0
フェーズII	60	7	25	15	4	9
フェーズI	35	5	13	6	6	5
合計	129	17	53	24	21	14

（2003 年 1 月時点）（文献 123 より許可を得て転載）

frame region (FR) をすべてヒト抗体に置き換えたものである[4] (Fig. 1)．以下に，マウスハイブリドーマ細胞から，遺伝子としてcDNAを用い遺伝子組換え法によるキメラ抗体，ヒト化抗体の作製法を紹介する．

第一のステップは，マウス抗体産生ハイブリドーマからのマウス抗体をコードする遺伝子（以下マウス抗体遺伝子）のクローニングである．ハイブリドーマ細胞よりRNAを抽出し，①cDNAを作製後，プラークハイブリダイゼーション法あるいはPCR法により抗体遺伝子をクローニングするか，②RNAより直接PCR法により抗体遺伝子をクローニングする方法が用いられている．ハイブリドーマ細胞は，目的の抗体遺伝子以外に，融合パートナーのミエローマ由来の抗体遺伝子，タンパク質に翻訳されない偽抗体遺伝子が含まれていることもある．

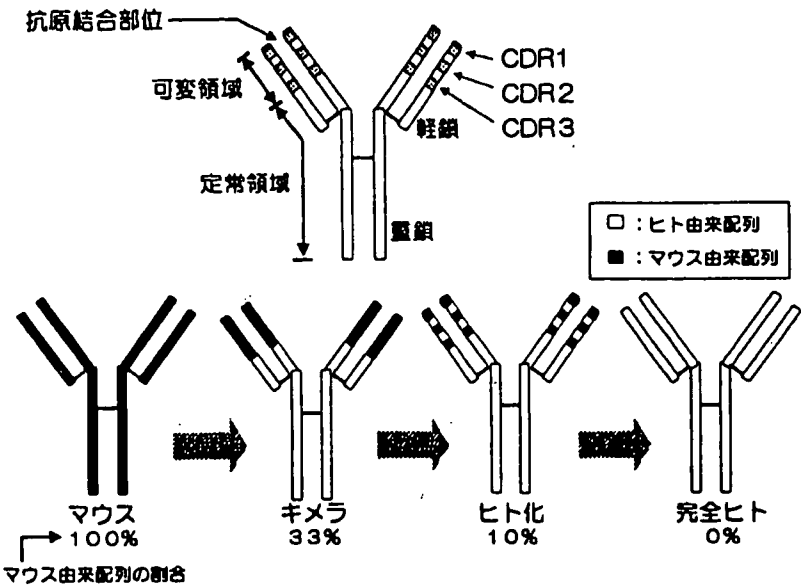

Fig. 1　抗体の構造（上段）及びマウスモノクローナル抗体のヒトに対する抗原性低減技術の進展（下段）
（文献 124 より許可を得て転載）

したがって，精製したモノクローナル抗体 V 領域のアミノ酸配列を一部決定し，クローニングした抗体遺伝子と一致しているか確認することが重要である．

キメラ抗体は，クローニングしたマウス抗体の variable（V）領域遺伝子にヒトの C 領域遺伝子を連結し，適当な発現ベクターに挿入して培養細胞で生産する．また，抗体産生ハイブリドーマのマウスイムノグロブリン（Ig）C 領域をヒト Ig C 領域に組換える相同組換え法やトランスジェニックマウスによっても作成される．

ヒト化抗体遺伝子の作製は以下の複雑なステップからなる．ヒト化抗体作製の第一ステップでは，クローニングしたマウス抗体可変（V）領域における抗原との結合に寄与する超可変領域（CDR）配列とヒト抗体 V 領域におけるアイソタイプ固有のアミノ酸配列をもつフレームワーク領域（FR）からなる V 領域をコードする遺伝子を構築する．ヒト化抗体作製における最も重要な点は，CDR を移植するヒト FR 領域のデザインである．マウス抗体の CDR を単純にヒト FR へ移植した抗体では，結合活性の低下，消失がみられる．これはマウス FR 領域中のいくつかのアミノ酸が CDR の高次構造維持に大きな影響を与えており，それらのアミノ酸残基を CDR とともに移植しなければいけないことを示している．CDR の高次構造に影響を与えるアミノ酸残基がいくつか同定されているが[5]，その法則は確立されておらず，コンピューターモデリングなどを組み合わせて個々の抗体で試行錯誤しているのが現状である[6]．また，この方策として目的のマウス抗体 V 領域と最も高いホモロジーを示すヒト抗体 V 領域を選択し，その FR 領域を用いている場合もある．

最終的に，構築された抗体 heavy（H）鎖及び light（L）鎖遺伝子が挿入された発現ベクターを動物細胞に導入し，遺伝子組換え抗体を発現する．現在，上市されている抗体の製造細胞で実績があるのは，チャイニーズハムスター卵巣由来の CHO 細胞，マウスミエローマ由来の NS0 細胞及び SP2/0 細胞である[7]．動物細胞が産生に用いられるのは以下の理由による．まず，抗体は H 鎖及び L 鎖各 2 本が複数の S-S 結合を介して結合しており，正確な立体構造の構築には動物細胞での発現が最適である．また，抗体の Fc 領域には N 型糖鎖が結合しており，糖鎖は C_H2 ドメインの立体構造の維持，後述する複数のエフェクター活性に必須である．したがって，動物細胞で発現しないと糖鎖が付加されないため，抗体のエフェクター活性が損なわれてしまうからで